Title: Dramatic Performance Gains in Vanadium Redox Flow Batteries Through Modified Cell Architecture

Authors: D.S. Aaron, Q. Liu, Z. Tang, G.M. Grim, A.B. Papandrew, A. Turhan, T.A. Zawodzinski, M.M. Mench

PII: S0378-7753(11)02445-1
DOI: doi:10.1016/j.jpowsour.2011.12.026
Reference: POWER 15184

To appear in: *Journal of Power Sources*

Received date: 7-9-2011
Revised date: 9-12-2011
Accepted date: 11-12-2011

Please cite this article as: D.S. Aaron, Q. Liu, Z. Tang, G.M. Grim, A.B. Papandrew, A. Turhan, T.A. Zawodzinski, M.M. Mench, Dramatic Performance Gains in Vanadium Redox Flow Batteries Through Modified Cell Architecture, {\it{Journal of Power Sources}} (2010), doi:10.1016/j.jpowsour.2011.12.026

Dramatic Performance Gains in Vanadium Redox Flow Batteries Through Modified Cell Architecture

D. S. Aaron[1], Q. Liu[1], Z. Tang[1], G. M. Grim[1], A. B. Papandrew[1], A. Turhan[1], T. A. Zawodzinski[1,2], M. M. Mench[1,2]

[1] BRANE Lab, University of Tennessee Departments of Chemical and Biomolecular Engineering and Mechanical, Aerospace and Biomedical Engineering, The University of Tennessee Knoxville, 37996

[2] Oak Ridge National Laboratory, Oak Ridge Tennessee, 37831

Submitted to the Journal of Power Sources as a Short Communication

August 28, 2011

Abstract

We demonstrate a vanadium redox flow battery with a peak power density of 557 mW cm^{-2} at a state of charge of 60%. This power density, the highest reported to date, was obtained with a zero-gap flow field cell architecture and non-wetproofed carbon paper electrodes. The electrodes were comprised of stacked sheets of carbon paper and optimized through systematic variation of the total electrode thickness. We anticipate significant reductions in the ultimate system cost of redox flow battery systems based on this design.

1. Introduction

Redox flow batteries (RFBs) are a potentially enabling technology for intermittent, renewable energy sources such as wind and solar power [1-3]. Large-scale energy storage in RFBs could alleviate the unpredictability of such energy sources by leveling their output over time [4-7]. One type of RFB is the all-vanadium redox battery, in which vanadium is dissolved in an acid solution, typically sulfuric acid. Since vanadium has four redox states, the V^{2+}/V^{3+} and V^{4+}/V^{5+} (present as VO^{2+}/VO_2^{+}) redox couples act as the negative and positive electrolytes, respectively. During discharge, V^{2+} is oxidized to V^{3+} while V^{5+} is reduced V^{4+}; charging a VRB reverses this process.

Much of the emphasis of recent research on vanadium redox batteries (VRBs) has focused on improving the energy density of the device. Indeed, conventional VRBs are limited in this regard, offering roughly 20 – 30 Wh L^{-1} (Li-ion batteries exceed 150 Wh L^{-1}) [8]. Work to increase this has focused on increasing the electrolyte concentration in the system. One important result of this work has been enabling wider operating temperatures along with the higher concentrations of vanadium species [9]. However, for most stationary power uses, the

energy density *per se* is a secondary consideration. Cost is a primary driver of applicability of these systems. Roughly speaking, key contributors to the installed cost of a VRB are the cost of the vanadium, the membranes used and everything else in similar proportion [10]. The vanadium cost is fixed by the required capacity and the purity of the vanadium feedstock demanded. The remaining costs are strong functions of the performance of the battery, best expressed as the power density or current density in the operating voltage range. The total area of cell and membrane represent a significant cost, which can be directly reduced by improving the power density. We note in passing that the operating cost of the system will be also be strongly influenced by the efficiency of operation. At the cell level, this is tantamount to increasing the operating voltage of the cell. This, in turn, also implies that the most rational path forward is to maximize the current density over a given voltage range, with a few other implications for the manner of operating the system.

In this work, we report the first in a series of efforts to increase VRB performance. Some rather slight changes in cell design and material selection enable a dramatic increase in power density of roughly five-fold over previously reported devices, with significant gains also achieved at a higher operating efficiency point.

2. Method of Approach

2.1 Cell construction

A modified direct methanol fuel cell (Fuel Cell Technologies) with 5 cm^2 active area was utilized in this work, as shown in Figure 1. To minimize ionic and contact resistances between the membrane and electrode, the RFB had a "zero-gap" configuration, meaning that the membrane, electrodes, and current collectors were in direct contact. A Nafion 117 (Ion-Power,

Inc.) membrane served as the separator. The electrodes were 10 AA carbon paper (SGL Technologies GmbH) with uncompressed thickness of ~410 μm and specific resistance of 0.012 Ω-cm. Poco pyro-sealed graphite plates with machined serpentine flow channels distributed the electrolyte across the active area of the RFB while also conducting current to gold-plated current collectors.

2.2 Electrolyte system

The all-vanadium electrolyte was initially made by dissolution of 1.0 M $VOSO_4$ (99.9% purity, Alfa Aesar) in a sulfuric acid solution with a total SO_4^{2-} concentration of 5 M. Both electrolyte reservoirs initially consisted of a solution containing only the V^{4+} ion. The positive electrolyte volume was initially 100 mL, twice the negative electrolyte volume. These electrolytes were then charged until the V^{4+} was converted to V^{2+} (negative electrode electrolyte) and V^{5+} (positive electrode electrolyte), and subsequently half of the positive electrolyte solution was removed from its reservoir, making the solution volumes equal. Acid-resistant diaphragm (KNF Lab) or peristaltic (Cole Parmer) pumps maintained a flow rate of 20 mL min^{-1} during charging. Nitrogen purging in the negative electrolyte reservoir was used to prevent the charged V^{2+} from oxidizing to V^{3+}.

2.3 Electrochemical measurements

Polarization curves and impedance spectroscopy were performed with a Bio-Logic HCP-803 potentiostat or a Scribner 857 potentiostat. The positive electrode of the battery served as the working electrode, while the counter and reference leads connected to the negative electrode. Discharging polarization curves were recorded galvanostatically, with the battery at an inital state of charge (SoC) of either 50% or 100%. The battery was assumed to be at full charge when

a current of < 20 mA (4 mA cm^{-2}) was observed when the battery was held potentiostatically at 1.8 V. A SoC of 50% was achieved by assuming 100% coulombic efficiency and discharging from 100% SoC at 500 mA for the appropriate time, based on the electrolyte volume and concentration. Each step in the polarization curves lasted for 30s. All experiments in this work occurred at room temperature with no active temperature control. However, the reservoir temperature did not measurably increase during an experiment, and the assumption of constant temperature is maintained throughout this work.

High frequency resistance (HFR) was measured at a single frequency in a range from 10 to 100 kHz with an AC perturbation of 10 mV amplitude. Areal specific resistance (ASR) was calculated by multiplying the HFR by the active area of the membrane, 5 cm^2. The ASR allowed us to correct polarization curves for ohmic (iR) losses at a given current density. The use of iR correction is noted where appropriate.

3. Results and Discussion

The critical difference between most designs reported in the literature and that described here is our use of a fuel cell-type structure with zero gap for electrolyte flow. We flow the solution through a flow field in contact with a porous carbon electrode. Flow into the electrode occurs by some combination of diffusion and convection perpendicular to the flow field path. It is possible that the use of a serpentine flow channel may introduce unacceptable pressure drops in installation-level cell hardware. If this is the case, the increased power density and efficiency realized by such a design, detailed below, may compensate for the increased parasitic pump load. A detailed analysis of system-level considerations such as these is beyond the scope of this contribution.

We used polarization curves to frame our analysis of the performance of the RFBs, as they help determine which processes dominate the overpotential at a particular current [11]. It is important to note that in a laboratory-scale flow battery, unlike in a fuel cell, a significant depletion of electrolyte capacity may occur during the measurement of a polarization curve. During our investigation of the optimized battery described below, the state of charge of the electrolytes was reduced from 100% to less than 35% when the limiting current density was reached. In this case, the peak power density was obtained when the SOC had been reduced to 60%. The state of charge of the battery has a significant effect on the maximum power density of the device. In the case of an initial state of charge of 50%, the peak power was reached at a state of charge of approximately 41%.

Figure 2 shows a comparison between the polarization curves of the optimized RFB and others found in the literature. Only one contribution [12] included a full polarization curve; the rest of the results were for partial polarization curves that had been used to calculate the internal resistance of a RFB. Additionally, the state of charge of these reported systems is seldom clearly defined. Nevertheless, the limiting current for our RFB with optimized electrode thickness exceeded 920 mA cm^{-2} at 0.20 V while the next highest was 280 mA cm^{-2} [12]. Moreover, the cell reported by Kjeang *et al.* [12] was of a microfluidic design that is not considered feasible for a large-scale energy storage application and showed small overall output. For a VRB with more similarities to our design, we found no published, complete polarization curves. However, the result from Chen *et al.* [13] shows an overpotential of 293 mV at 20 mA cm^{-2} compared to 70 mV at the same current for our RFB. The state of charge of the device in Ref. [13] is not stated explicitly; our device was at nearly full charge. However, we found the overpotentials in our

system at 20 mA cm^{-2} were unchanged at an initial state of charge of 50%. The design we report here thus offers increased efficiency over the entire range of operational current density.

The use of a zero-gap cell architecture and thin electrodes had a pronounced effect on the ohmic losses in the cell. An ASR of 0.50 Ω-cm^2 was found for the VRB reported here, while the ASR values reported by Chen (13) and Kazacos (14) were 3.5 Ω-cm^2 and 5.4 Ω-cm^2, respectively. Irrespective of any other losses, a VRFB with an OCV of 1.5 V and an ASR of 5 Ω-cm^2 will never be capable of sustaining more than 300 mA cm^{-2}, and in service will be limited to even lower current density in order to deliver a useful cell voltage. In contrast, a battery with an ASR of 0.50 Ω-cm^2 is limited to 3 A cm^{-2}. Of course, other losses are present, and this is plainly evident in the nonlinearity of the polarization curves we present. Nevertheless, lowering the ohmic ASR of a battery is a prerequisite for increasing its maximum current and power density.

Elimination of any gap between the membrane and the electrodes, a substantial reduction in electrode thickness, and a significant compressive load on the cell are all likely contributors to the reported reductions in ohmic ASR. These modifications respectively reduce the ionic, electronic, and contact resistances in the electrode, and when taken together have a large overall effect on the total cell ASR.

While high power density is desirable and often an important metric of RFB performance, overpotential is an essential consideration as well. Improved power density can lead to reduced costs, as less material would be needed to support a desired power output. However, the overpotential is also quite large at high power, resulting in relatively inefficient operation. This inefficiency, manifested as waste heat, can also introduce stack thermal control issues. Thus, efforts to improve RFBs can also focus on maximizing current at a relatively low overpotential

(i.e. a practical voltage efficiency) rather than pushing out the limiting current to greater values. In this regard, we have made nearly five-fold improvements in current density at 1.2 V. Nonetheless, documenting the peak power provides more complete information to contribute to the optimization. Also, higher performance near the peak power point provides a wider operating range for the same device, i.e. a larger ratio between peak power and power at a typical high efficiency operating point. This provides a bit more flexibility in sizing a battery if substantial short-term fluctuation of power demand or peak shaving ability is present in the system to which storage is added.

We focused on increasing RFB performance by probing the influence of electrode thickness on polarization losses in the cell. A key trade-off associated with thicker electrodes is between the enhancement of the available surface area for the electrochemical reaction and the penalties associated with poorer mass transport through a thicker layer. We systematically varied the thickness of one electrode by stacking multiple layers of carbon paper on top of one another, while retaining a single layer of carbon paper as the conjugate electrode. Figures 3 and 4 show iR-free polarization curves from RFBs initially at 100% SoC for which the number of layers of carbon paper comprising the negative and positive electrodes, respectively, was varied from 1 to 3. In all cases, the electrode compression was 19 - 25% when the RFB was assembled.

On the negative electrode, multiple layers were superior (i.e. lower overpotential) to a single-layer, though three layers performed worse than two layers (Figure 3). The overpotentials at 20 mA cm^{-2} (in the activation dominated polarization region) for one, two and three layers of negative electrode were 98, 83, and 113 mV, respectively. The best performance in the ohmic and mass transport-limited regions was observed with two negative electrode layers, as well, with the difference more pronounced than at low current. There is clearly an important interplay

between the kinetic losses which scale with the available electrode surface area and the ohmic losses in the electrolyte solutions, which are a function of the convective and diffusive flow to and from the electrode. Different electrode materials will clearly impact this balance.

Figure 4 shows results for one to three layers of positive electrode carbon paper and a single negative electrode layer. In this case, multiple layers were again superior to a single electrode layer; however, three positive electrode layers performed slightly better than two, especially at greater current. At 20 mA cm^{-2}, two layers again exhibited the least overpotential – the overpotentials were 98, 68, and 109 mV for one, two and three positive electrode layers, respectively. Above 520 mA cm^{-2}, however, the three-layer setup exhibited less iR-free overpotential than the two-layer setup.

Based on these results, we attempted to construct an optimized RFB employing two layers of carbon paper as the negative electrode and three layers as the positive electrode, since these exhibited the lowest overpotentials individually. However, this configuration did not result in the best performance. We found instead that a configuration using three layers of carbon paper to form each electrode was superior. This illustrates the importance of single-electrode studies, which we are presently conducting with the aid of a recently developed *in situ* reference electrode [15].

Figure 5 compares the iR-free polarization curves from the optimized RFB to the single-layer case at a starting SoC of 100%.

5. Conclusions

In this work, the maximum reported power density of a vanadium redox flow battery was increased more than five-fold compared to other conventional published systems. We attribute

this primarily to the zero gap flow field architecture and thin carbon paper electrodes that ensured good contact between all components of the cell and reduced charge transport distances. In addition, the presence of a serpentine flow field effectively spread the electrolyte across the entire membrane surface area, enhancing mass transport to the electrodes. Utilization of multiple electrode material layers as the negative and positive electrodes also resulted in improved flow battery output, and demonstrated the coupled nature of ohmic, kinetic, and mass transport losses in these systems. The results of this study provide a pathway forward to reduced cost and dramatically improved performance in vanadium redox flow battery systems.

Acknowledgements

This work was partially funded by the Experimental Program to Stimulate Competitive Research (EPSCoR) under NSF grant EPS-1004083. Partial support of this work was also provided though NSF Early Career Development Award # 0644811.

References

[1] M. Rychick, M. Skyllas-Kazacos, Journal Of Power Sources 22 (1988) 59-67.

[2] M. Skyllas-Kazacos, D. Kasherman, D.R. Hong, M. Kazacos, Journal Of Power Sources 35 (1991) 399-404.

[3] R. Dell, Journal Of Power Sources 100 (2001) 2-17.

[4] L. Joerissen, J. Garche, C. Fabjan, G. Tomazic, Journal Of Power Sources 127 (2004) 98-104.

[5] C. Ponce de Leon, A. Frias-Ferrer, J. Gonzalez-Garcia, D. Szanto, F.C. Walsh, Journal Of Power Sources 160 (2006) 716-732.

[6] C. Fabjan, J. Garche, B. Harrer, L. Jorissen, C. Kolbeck, F. Philippi, G. Tomazic, F. Wagner, Electrochimica Acta 47 (2001) 825-831.

[7] Z. Yang, J. Zhang, M. Kintner-Meyer, X. Lu, D. Choi, J. Lemmon, J. Liu, Chemical Reviews 111 (2011) 3577 – 3613.

[8] M. Skyllas-Kazacos, G. Kazacos, G. Poon, H. Verseema. International Journal of Energy Research 34 (2010) 182-189.

[9] J. Zhang, L. Li, Z. Nie, B. Chen, M. Vijayakumar, S. Kim, W. Wang, B. Schwenzer, J. Liu, Z. Yang, Journal of Applied Electrochemistry, DOI: 10.1007/s10800-011-0312-1

[10] M. Moore, R. Counce, J. Watson, T. Zawodzinski, H. Kamath Chemical Engineering Education, submitted

[11] D. Aaron, Z. Tang, A. Papandrew, T. Zawodzinski, Journal of Applied Electrochemistry, 41, (2011) 1175

[12] Kjeang, E., R. Michel, D. Harrington, N. Djilali, D. Sinton, Journal of the American Chemical Society 130 (2008) 4000 – 4006.

[13] D. Chen, S. Wang, M. Xiao, Y. Meng, Journal of Power Sources 195 (2010) 2089-2095.

[14] M. Kazacos, M. Skyllas-Kazacos, Journal of the Electrochemical Society, 136 (1989) 2759

[15] D. Aaron, T. Zhijiang, J. Lawton, A. B. Papandrew and T. A. Zawodzinski, ECS Trans., in press. (2011)

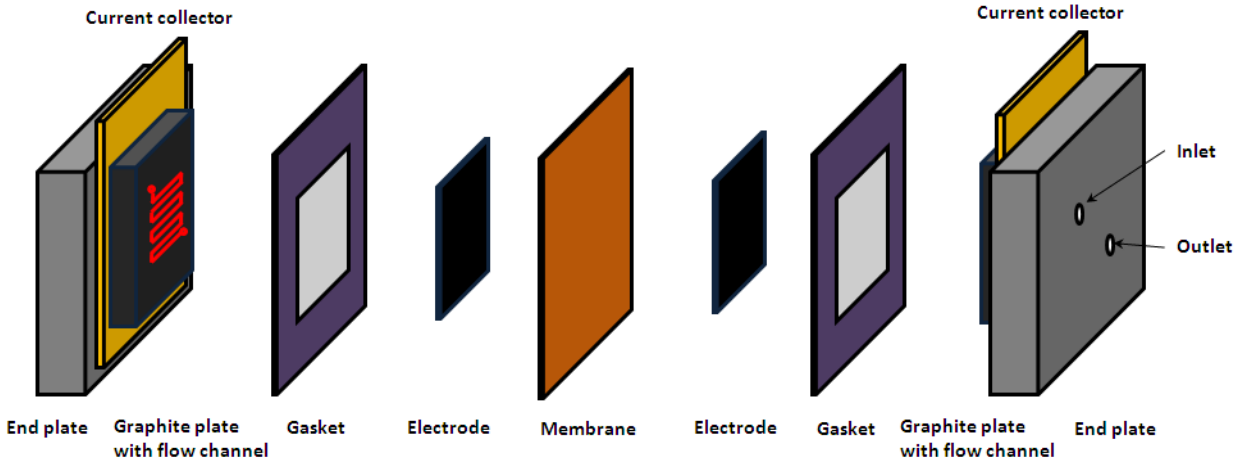

Figure 1: Picture/Schematic of VRB test setup in the BRANE lab.

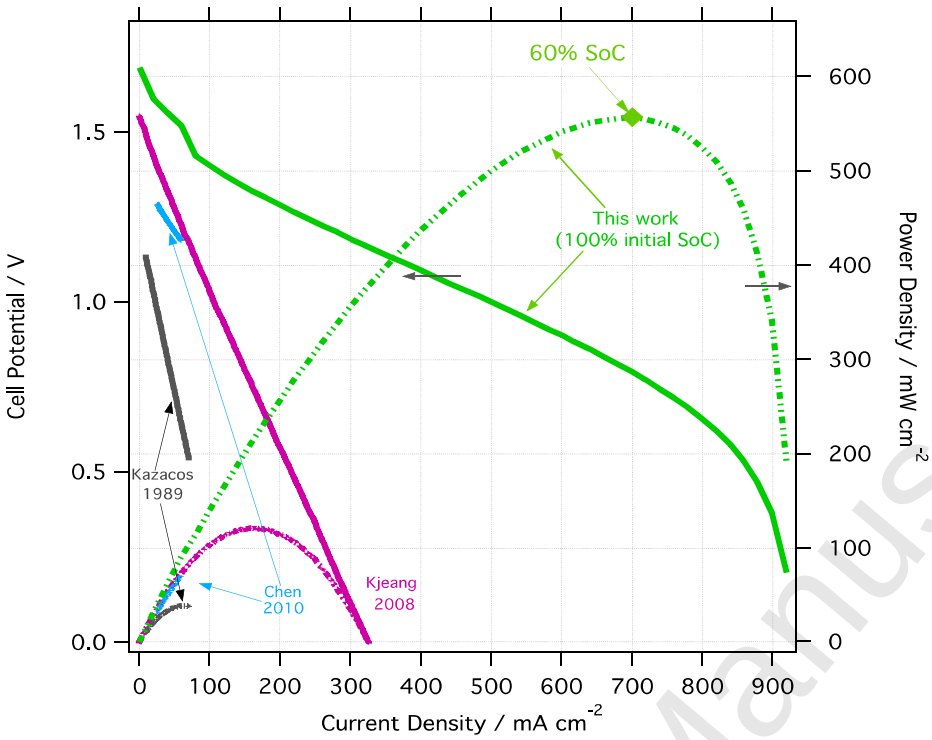

Figure 2: Performance curves of single layer electrode versus other published work. Solid lines are power density; dotted lines are cell potential. Our work was performed with 1 M vanadium in 4 M H_2SO_4 and 50% state of charge.

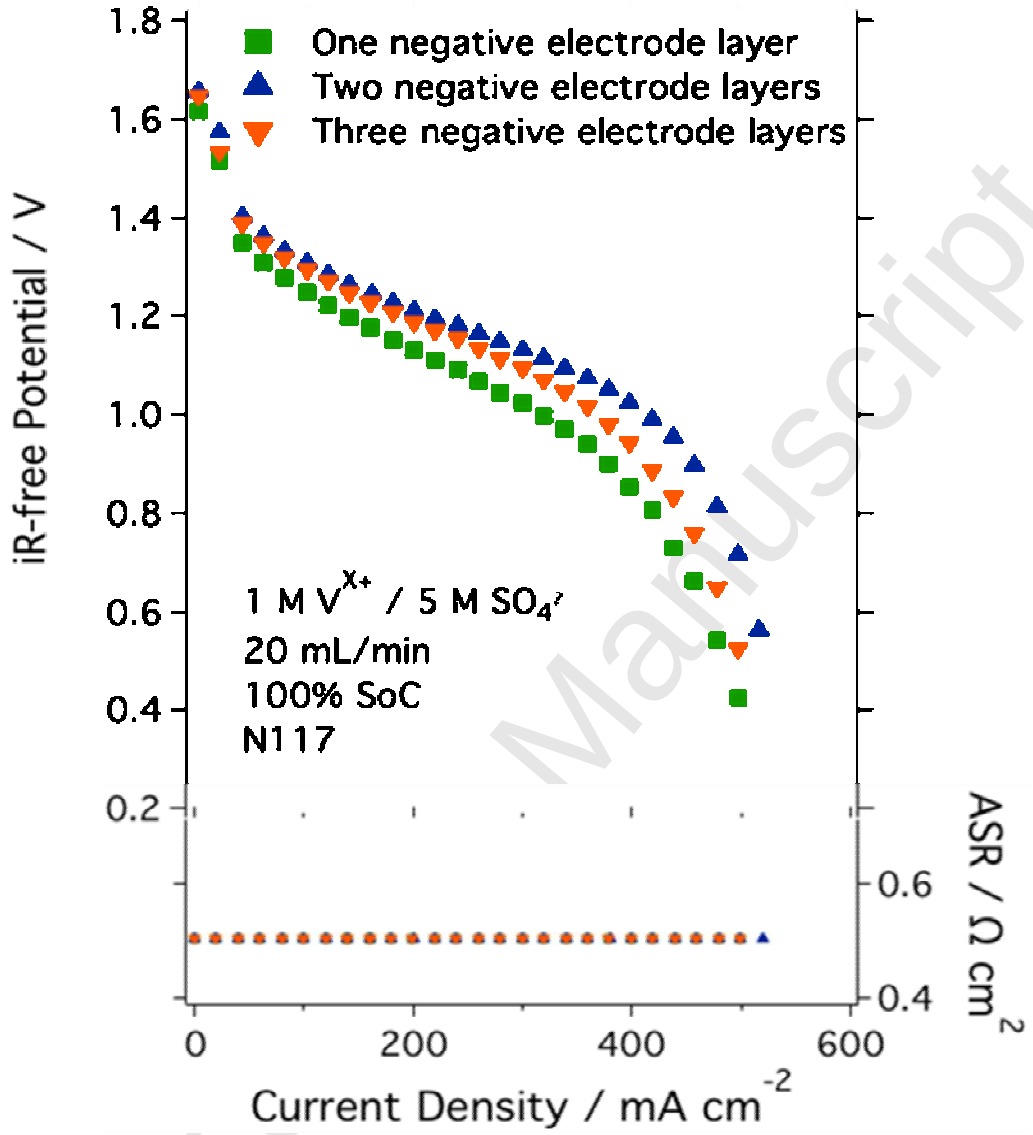

Figure 3. iR-free polarization curves showing the effect of number of negative electrode layers on RFB performance. The positive electrode was a single layer of carbon paper for each experiment.

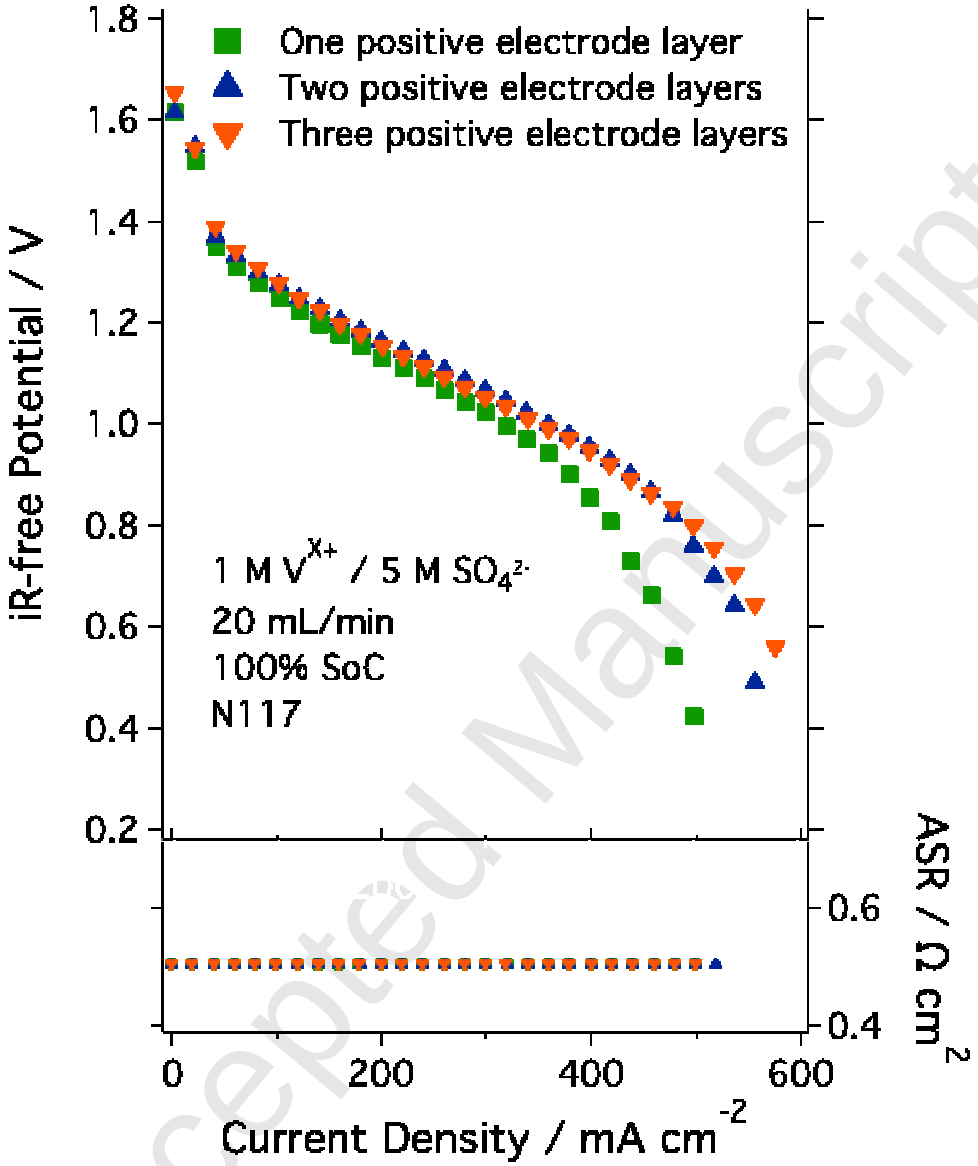

Figure 4. iR-free polarization curves showing the effect of varying positive electrode layers on RFB performance. The negative electrode was a single layer of carbon paper for each experiment.

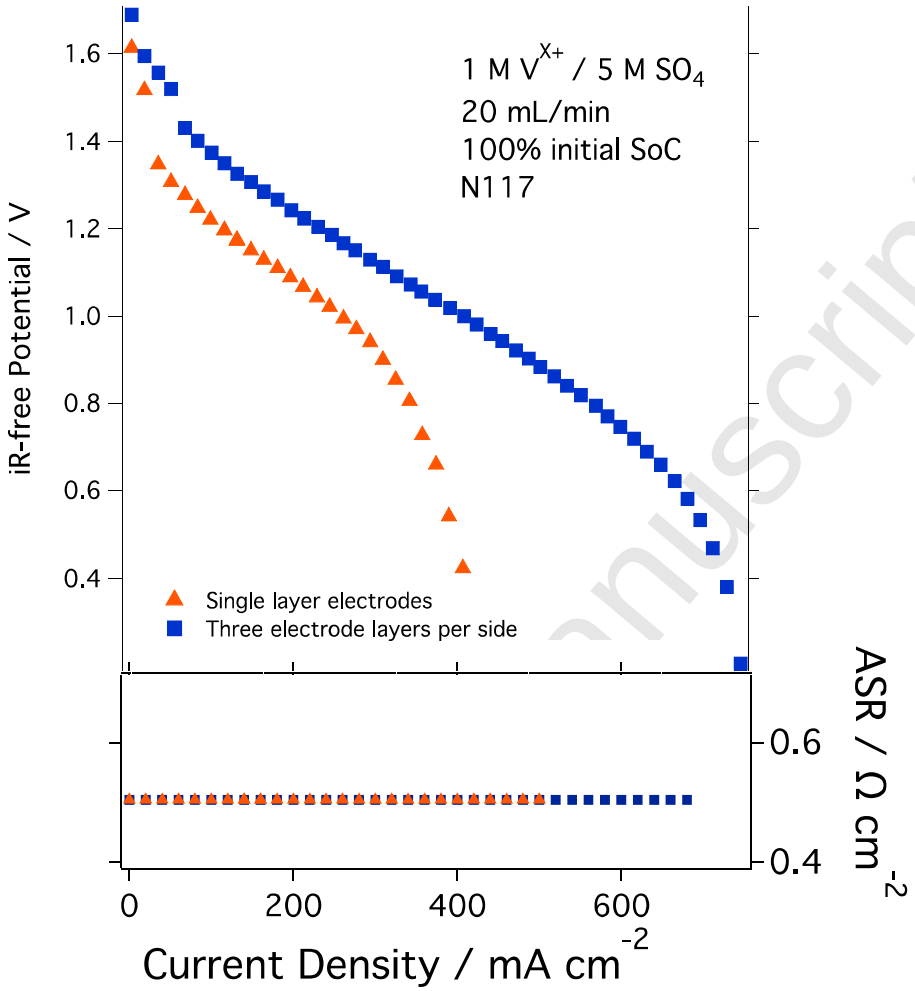

Figure 5. iR-free polarization curve comparison between "optimized" electrode layers and single electrode layers.

Highlights

- The MR phenomenon is observed in BCMCO sample in the FC magnetization measurement as the applied field is below 1030 Oe.
- The presence of two components to the magnetic ordering come from the contribution of Mn^{3+}/Mn^{4+} and Cr^{3+}moments.
- The MR phenomenon is suggested to stem from the antiparallel coupling of the Cr^{3+} moments and the canted $Mn^{3+/4+}$ moments.